Hao, Le; Cuesta, Francisco S.; Tretyakov, Sergei A.; Rupp, Markus

Improving Propagation Channels With Static Scatterers

Published in:
IEEE Antennas and Wireless Propagation Letters

DOI:
10.1109/LAWP.2024.3374419

Published: 04/06/2024

Document Version
Publisher's PDF, also known as Version of record

Published under the following license:
CC BY

Please cite the original version:
Hao, L., Cuesta, F. S., Tretyakov, S. A., & Rupp, M. (2024). Improving Propagation Channels With Static Scatterers. *IEEE Antennas and Wireless Propagation Letters*, *23*(6), 1924-1928.
https://doi.org/10.1109/LAWP.2024.3374419

Improving Propagation Channels With Static Scatterers

Le Hao, *Student Member, IEEE*, Francisco S. Cuesta, Sergei A. Tretyakov, *Fellow, IEEE*, and Markus Rupp, *Fellow, IEEE*

***Abstract*—This letter explores the potential enhancement of radio signal propagation in intricate environments through the deployment of basic resonant dipole scatterers. We employ the MATLAB ray tracer algorithm to examine the impact of dipolar scatterers on the power received at the user's location. The ray tracing model is modified for a dipolar scatterer model based on its bi-static scattering cross-section. Our analytical and simulation results indicate that the deployment of extra scattering components is nearly ineffective when a direct link is present. Conversely, in scenarios where there is no line-of-sight, the proposed approach can considerably boost the power delivered. This cost-effective and straightforward method could complement other channel optimization strategies, such as the application of reconfigurable intelligent surfaces.**

***Index Terms*—Channel optimization, dipolar scattering, ray tracing.**

I. Introduction

IN WIRELESS communication systems, passive structures are a promising technology for expanding coverage, enhancing signals, and compensating for blind zones [1], [2]. For example, reconfigurable intelligent surface (RIS) technology has been widely studied due to its adaptive functionalities [3]. Other techniques, such as fully passive metal reflectors, are also attractive since their energy consumption is zero and they are compatible with existing and future wireless systems [4].

However, either using an RIS or a metal reflector requires the plate to be oriented in such a way that the scattered beams point towards the desired user. In addition, metal plates produce specular reflection, in other words, a signal can only be received when the observation angle is close to the incident angle. Therefore, these approaches are not universal and may be inconvenient, involving human control or complex algorithms.

According to the power scaling law derived for an abstract model of noninteracting and fully controllable array elements [5], with an untuned RIS (not optimized for any desired direction), the received power at the user can achieve a 3 dB gain when doubling the RIS element number [6]. Inspired by this concept, we aim to find other more convenient and realistic alternatives that can improve the received power by the user without extra control from humans. In fact, we find that just randomly deploying multiple resonant dipoles as scatterers in the environment can achieve similar results as expected for such models of an untuned RIS. Since the radiation pattern of a dipole is omnidirectional in the azimuthal plane, users at any azimuth angles could be served by the dipole scatterers regardless of their position.

To the best of the authors' knowledge, there are no studies on improving propagation channels using such static scatterers and no studies on analyzing such static scatters with ray tracing tools. The closest work from the literature is using a fully passive metallic plate as a reflector [4]. However, as mentioned before, metal plates mostly produce specular scattering and any modification in the desired reflection direction would require manual reorientation of the plate. Untuned RISs also give some diffuse scattering, but their effect is less pronounced due to the nonresonant response of array elements loaded by random loads. In contrast, in the proposed clusters of weakly coupled dipoles, scattering from each dipole is maximized, as they act at the resonance.

In this letter, we explore in which scenarios it is beneficial to implement static scatterers and in which scenarios they do not offer significant improvements. In addition, we investigate how much improvement the user can receive through randomly located scatterers and what parameters have a high impact. We explore the contribution of these scatters in indoor and outdoor scenarios using the MATLAB ray tracer algorithm. The rest of this article is organized as follows. Section II introduces the path-loss model. Section III provides numerical simulation results from indoor and outdoor scenarios. Finally, Section IV concludes this letter.

II. Received Power Calculation

We use resonant dipoles (for example, half-wave metal wire or strip dipoles) as scatterers since they are low-cost, very simple to implement, and have an omnidirectional radiation pattern in the azimuthal plane. By placing multiple dipoles randomly in the environment, we can achieve random phases of waves scattered from them. When a dipole with its load is at resonance and there is no resistive loss, the scattered power is maximized [7]. In this case, the scattering cross-section of the dipole is $\sigma_{\max} = 4A_eG$, where A_e is the effective area, and G is the gain of the dipole. When the dipole load is conjugate-matched, $\sigma_{\text{match}} = A_eG$ [8]. Therefore, in this letter, we use short-circuited resonant dipoles to scatter as much power as possible.

Manuscript received 22 February 2024; accepted 5 March 2024. Date of publication 7 March 2024; date of current version 4 June 2024. This work was supported in part by the European Union's Horizon 2020 research and innovation programme under the Marie Skłodowska-Curie Grant 956256, in part by the Academy of Finland under Grant 345178, and in part by TU Wien Bibliothek through its Open Access Funding Programme. *(Corresponding author: Le Hao.)*

Le Hao and Markus Rupp are with the Institute of Telecommunications, Vienna University of Technology, 1040 Vienna, Austria (e-mail: le.hao@tuwien.ac.at; markus.rupp@tuwien.ac.at).

Francisco S. Cuesta and Sergei A. Tretyakov are with the Department of Electronics and Nanoengineering, Aalto University, 00079 Aalto, Finland (e-mail: francisco.cuestasoto@aalto.fi; sergei.tretyakov@aalto.fi).

Digital Object Identifier 10.1109/LAWP.2024.3374419

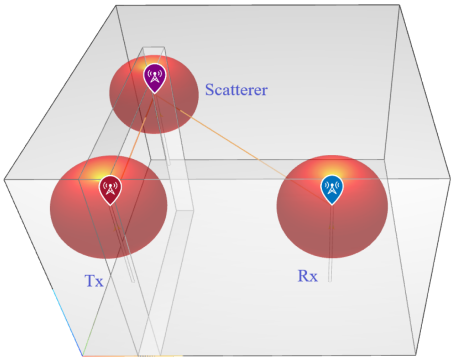

Fig. 1. SISO scenario with 3 dipoles being the Tx, Rx, and the scatterer.

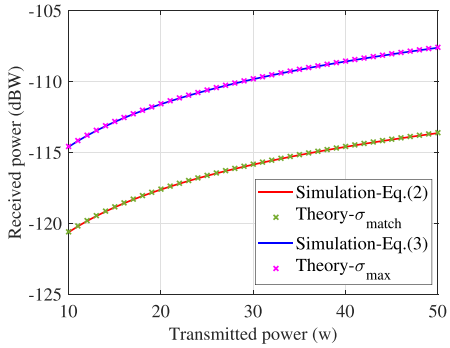

Fig. 2. Comparison of ray tracing simulation results and theoretical results.

By applying the definition of the scattering cross-section, we can infer that the transmitted power is first captured by the target and subsequently reradiated isotropically. The power delivered to the receiver load P_r is calculated by the radar range [9]

$$P_r = \frac{P_t G_t G_r \sigma \lambda^2}{64\pi^3 (R_1 R_2)^2} \tag{1}$$

with P_t being the transmit power and σ the radar cross-section of the scatterer. Furthermore, G_t and G_r are the gains of the transmitting (Tx) and the receiving (Rx) antennas, respectively. R_1 and R_2 denote the distances between the Tx and the scatterer, and between the scatterer and the Rx antenna, respectively. However, this model considers a free-space scenario, with only one line-of-sight (LoS) path between the Tx antenna and the scatterer, and between the scatterer and the Rx antenna. In a real environment, the multipath propagation through reflections cannot be ignored. Therefore, we use the MATLAB ray tracer to obtain more accurate received power, which takes the reflection from the environment and losses due to the types of reflection materials into account.

The MATLAB ray tracer calculates the received power at the Rx antenna from each propagation path as

$$P_r = P_t \frac{G_t G_{\text{rx}} \lambda^2}{(4\pi R_1)^2} \frac{G_{\text{tx}} G_r \lambda^2}{(4\pi R_2)^2} = \frac{P_t G_t G_r G_{\text{tx}} G_{\text{rx}} \lambda^4}{(4\pi)^4 (R_1 R_2)^2} \tag{2}$$

with G_{tx} and G_{rx} being the gain of the scatterer when it is in the Tx and Rx modes, respectively. However, (2) is based on the Friis formula, and it holds the assumption that the load of the scattering antenna is conjugate-matched. As discussed above, in that case, the scattered power is not at its maximum, because the currents flowing at the antenna body are weaker if there is a resistive load. Basically, (2) corresponds to the radar-range (1) where $\sigma = \sigma_{\text{match}}$.

Since the difference of σ for lossless resonant and conjugate-matched dipoles is the factor of four, the correct model from ray tracing should be

$$P_r = \frac{4 P_t G_t G_r G_{\text{tx}} G_{\text{rx}} \lambda^4}{(4\pi)^4 (R_1 R_2)^2}. \tag{3}$$

To verify this model, we set up a simple scenario as shown in Fig. 1 and use the MATLAB ray tracer to calculate the received power. In the simulation, we use a resonant dipole as a Tx and Rx antenna, and the same dipole as a scatterer. The resonant frequency is 30 GHz, and the maximum gain of the dipole is 2.1 dB. According to the relation between the antenna gain and the effective area $A_e = G\lambda^2/(4\pi)$, we can calculate $\sigma_{\text{max}} = 4A_e G = 4\tilde{}G^2\lambda^2/(4\pi) = 0.8372\lambda^2$ and $\sigma_{\text{match}} = A_e G = G^2\lambda^2/(4\pi) = 0.2093\lambda^2$.

In the scenario where the Tx and Rx antennas are blocked, there is only one LoS path between Tx and the scatterer and one LoS path between the scatterer and the Rx. For the distances $R_1 = 2$ m and $R_2 = 2.8$ m, the received power from (1) with $\sigma = \sigma_{\text{max}}$ and $\sigma = \sigma_{\text{match}}$, (2), and (3) are shown in Fig. 2. The results show that the original ray tracing model from (2) gives the same results as if we use $\sigma = 0.2093\lambda^2$ in (1). The modified ray tracing model from (3) gives the same results as the correct theoretical model from (1) with $\sigma = 0.8372\lambda^2$. In the following simulations, we use the modified ray tracing model to calculate the received power at the Rx antenna.

It is worth noting that (3) is applicable when there is only one LoS path for the Tx-scatterer and scatterer-Rx links. When considering multipath reflections from the environment, the reflection losses due to different material types are also included in the path loss calculation in the MATLAB ray tracer. The final received power at the Rx antenna can be classified as from the direct link, i.e., from the Tx antenna to the Rx antenna only through wall reflections, and from the dipole-assisted link, that is, the transmit signals reflected by dipoles and then reaching the Rx antenna. There are also wall reflection paths from the Tx antenna to the dipole and from the dipole to the Rx antenna in the dipole-assisted link.

The received power at the Rx antenna from Tx through wall reflections is denoted as P_d. The received power from all the dipoles is denoted as P_{dip}, and the total received power from both the direct link and from all dipoles is written as P_{tot}. The contribution due to the dipoles is denoted as $\gamma = P_{\text{tot}}/P_d$, where $P_{\text{tot}} = P_d + P_{\text{dip}}$. Assuming that there are in total L paths in the direct link, P_d is calculated in the MATLAB ray tracer as

$$P_d = P_t \left| \sum_{l=1}^{L} \sqrt{\frac{G_t G_r}{\text{PL}_d^{(l)}}} e^{j\theta_d^{(l)}} \right|^2 \tag{4}$$

where $\text{PL}_d^{(l)}$ is the path loss of the lth path that includes the free-space path loss and the reflection loss from the walls

$$\text{PL}_d^{(l)} = \left(4\pi R_d^{(l)}/\lambda\right)^2 \alpha^{(l)} \tag{5}$$

where $R_d^{(l)}$ is the propagation distance for the lth path, and $\alpha^{(l)}$ is the reflection loss for the lth path. The phase shift of the lth path is denoted as $\theta_d^{(l)}$.

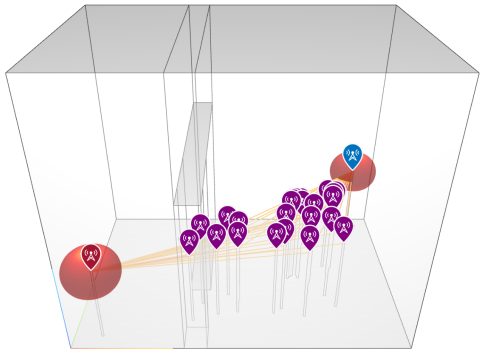

Fig. 3. Two-room scenario with 23 dipoles. The red, blue, and purple markers represent the Tx, Rx, and dipoles, respectively.

Similarly, we assume there are in total K dipoles and M_k and N_k reflection paths between the Tx antenna and the kth dipole and between the kth dipole and the Rx antenna, respectively. The received power at the kth dipole from the Tx antenna is calculated as

$$P_t^{(k)} = P_t \left| \sum_{m_k=1}^{M_k} \sqrt{\frac{G_t G_{\text{rx}}}{\text{PL}_t^{(m_k)}}} e^{j\theta_t^{(m_k)}} \right|^2. \tag{6}$$

Since the dipoles are lossless, all the captured power is scattered into space. The received power at the Rx antenna from the kth dipole is obtained by

$$P_r^{(k)} = P_t^{(k)} \left| \sum_{n_k=1}^{N_k} \sqrt{\frac{G_{\text{tx}} G_r}{\text{PL}_r^{(n_k)}}} e^{j\theta_r^{(n_k)}} \right|^2 \tag{7}$$

where $\theta_t^{(m_k)}$, $\theta_r^{(n_k)}$, $\text{PL}_t^{(m_k)}$, and $\text{PL}_r^{(n_k)}$ denote the phase shifts and the path loss of the m_kth path from the Tx to the dipole and the n_kth path from the dipole to the Rx antenna, respectively. The path loss factors $\text{PL}_t^{(m_k)}$ and $\text{PL}_r^{(n_k)}$ are obtained similarly as in (5) and include both the free-space path loss as well as the reflection loss. The total received power from all K dipoles is calculated as

$$P_{\text{dip}} = \sum_{k=1}^{K} 4P_r^{(k)}. \tag{8}$$

The factor of four in (8) is the correction factor for the radar cross-section of a lossless resonant dipole, see (3). In the above equations, since $G_{\text{tx}} = G_{\text{rx}}$ for reciprocal scatterers, we do not add subscripts for each dipole.

III. Ray Tracing Simulations

A. Indoor Scenario With a Strong Direct Link

First of all, we set up a MATLAB ray tracer simulation of a two-room scenario, as shown in Fig. 3. A big room with the size of $6 \times 4 \times 5$ m^3 corresponding to the length $\times$ width $\times$ height is separated from a small room ($2 \times 4 \times 5$ m^3 and $3.6 \times 4 \times 5$ m^3) by an open door in between. The Tx and Rx antennas are located in different rooms. Between them, there are 23 randomly placed dipoles. The heights of the Tx, Rx, and the dipoles are all 1.5 m. The dipoles and the Tx and Rx antennas are all in the far-field of each other. There are no LoS paths between the Tx and Rx antennas, but there are strong reflection paths from the walls that can reach the Rx antenna. Each dipole has LoS connections with both the Tx and Rx antennas.

TABLE I
Results With One Reflection and Different Material Types

Material	Concrete	Plasterboard	Wood	Ceiling board
P_d (dB)	-81.2658	-83.7207	-86.5063	-89.9846
P_{dip} (dB)	-114.4580	-115.1207	-115.3476	-115.3150
P_{tot} (dB)	-81.2637	-83.7176	-86.5006	-89.9719
γ (dB)	0.0021	0.0031	0.0057	0.0127

TABLE II
Results With Three Reflections and Different Material Types

Material	Concrete	Plasterboard	Wood	Ceiling board
P_d (dB)	-82.1522	-85.0051	-87.8605	-90.9118
P_{dip} (dB)	-114.0701	-115.1212	-115.4183	-115.3106
P_{tot} (dB)	-82.1494	-85.0009	-87.8529	-90.8961
γ (dB)	0.0028	0.0042	0.0076	0.0157

TABLE III
Results With One Reflection and Different Frequencies

Frequency (GHz)	10	30	60
P_d (dB)	-84.6241	-89.9846	-93.3166
P_{dip} (dB)	-95.5249	-115.3150	-127.0857
P_{tot} (dB)	-84.2848	-89.9719	-93.3148
γ (dB)	0.3393	0.0127	0.0018

When considering the reflections from the environment, different wall materials can cause different reflection losses. Therefore, we set the material as "concrete," "Plasterboard," "wood," and "ceiling board," respectively, to observe their influences. The simulation results with one reflection and three reflections are displayed in Tables I and II, respectively. From both tables, we can observe that the direct link contributes much stronger power than the dipole-assisted link. In this case, the contribution from the dipoles is seen to be insignificant. The results with three reflections are better compared with the one reflection scenario due to more propagation paths, but the difference is not so significant since there are many destructive paths from the wall reflections. From the comparison of the four different materials, we find that the material loss from the lowest to the highest is concrete $<$ plasterboard $<$ wood $<$ ceiling board. The higher improvement from the dipoles can be seen when the material loss is higher.

Next, we run simulations within the same scenario at the frequencies of 10–60 GHz and set the material type as "ceiling board" to compare the results with one reflection. The results are given in Table III. It is evident that at lower frequencies the received power is higher than at higher frequencies. The contribution from the dipoles at a lower frequency is also stronger than at a higher frequency. Hence, it is more useful to place scatterers in lower frequency systems than at higher frequencies.

B. Indoor Scenario Without a Direct Link

In this section, we simulate a library scenario as shown in Fig. 4, where the direct link is totally blocked by four high shelves inside the room. The Tx and Rx antennas are placed at the two ends of the room, and several dipoles are randomly placed in the corridor. The material of this scenario is set as "wood," and we set three reflections in the simulation. It should be noted that, in this scenario, no reflection paths from the Tx antenna can reach the Rx antenna, even if we set the reflection

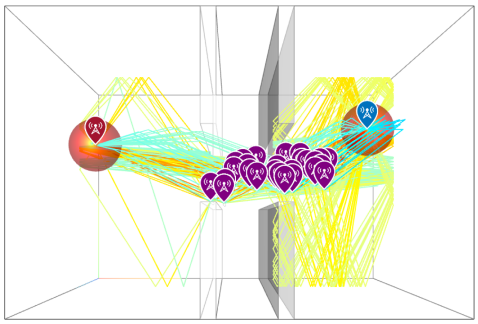

Fig. 4. Library scenario with the direct link being blocked. The red, blue, and purple markers represent the Tx, Rx, and dipoles, respectively.

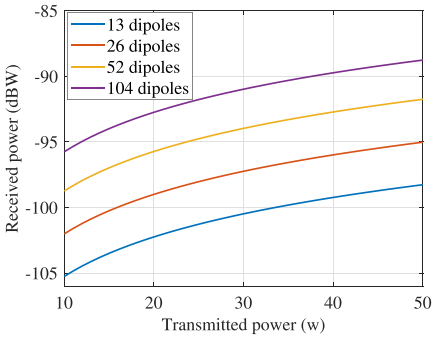

Fig. 5. Received power results with different numbers of dipoles in an indoor scenario.

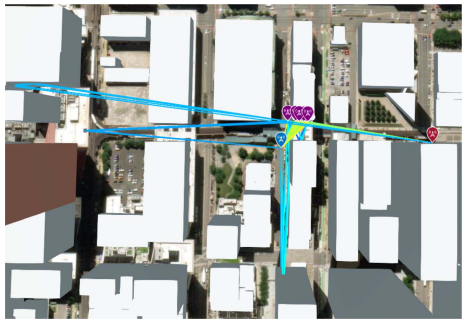

Fig. 6. Outdoor scenario with the direct link being blocked. The red, blue, and purple markers represent the Tx, Rx, and dipoles, respectively.

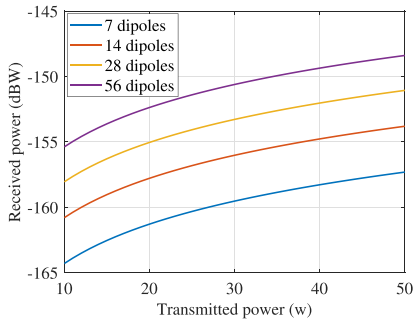

Fig. 7. Received power results with different numbers of dipoles in an outdoor scenario.

number as six or higher. This refers to a completely blinded spot where the Rx antenna can only receive signals through the dipolar scatterers. Hence, the number of dipoles plays a key role in this scenario.

We set the number of dipoles as 13, 26, 52, and 104 to observe the received power at the Rx antenna. The results are displayed in Fig. 5. The simulation results show 3.24, 3.27, and 2.99 dB difference when the number of dipoles increases from 13 to 26, from 26 to 52, and from 52 to 104, respectively. Compared with the results for a model of an untuned RIS in [10], the received power improvement seen here is very close to 3 dB when doubling the number of dipoles. The reason for this agreement is that the model of an untuned RIS in [10] neglected field interactions between the RIS elements, which is a reasonable assumption for the studied case of randomly positioned dipoles.

C. Outdoor Scenario Without a Direct Link

In this section, we run ray tracing simulations in an outdoor scenario: the Chicago city exported from OpenStreetMap. The setup is shown in Fig. 6, in which we place the Tx and Rx antennas next to two buildings and place several dipoles on the street where the scattered waves can reach both the Tx and the Rx antennas. However, there is no reflection path between the Tx and the Rx antenna, i.e., the Rx antenna can only receive signals through the dipolar scatterers. It should be noted that the Tx and Rx antennas are all the same as the dipoles we placed on the street as static scatterers. The heights of them are also the same. In the simulation, we set three reflections for both the Tx-dipoles and dipoles-Rx links and vary the number of dipoles to be 7, 14, 28, and 56. The received power results for different numbers of dipoles are shown in Fig. 7. The power difference between 14 and 7 dipoles is 3.51 dB. The difference between 28 and 14 is 2.74 dB, and the difference between 56 and 28 is 2.67 dB. It is found that the power difference with doubled dipole numbers is also close to 3 dB, but it has more deviations compared with the indoor scenario. In addition, when the number of dipoles increases, the differences get smaller. This is a more realistic situation because when the number of scatterers gets larger and larger, the gain cannot always increase by the same amount. Otherwise, the gain would reach infinity when the scatterer number grows infinitely, which is obviously wrong. From the comparison between the indoor and the outdoor scenario, we can conclude that the improvement due to the increase of the dipole numbers is higher in a rich scattering environment than in a sparse scattering environment.

IV. Conclusion

In this contribution, we consider the possibility of using static resonant dipole scatterers in the propagation environment to improve the received power at the Rx antenna. We modify the ray tracing model based on the bi-static scattering cross-section of a short-circuited resonant dipole. Then, we use the MATLAB ray tracer to simulate the received power at the Rx antenna through the dipoles including multiple reflections in the environment. We compare the results with different reflection materials, different frequencies, and different numbers of dipoles. The simulation results prove that in a scenario with a strong direct link, placing scatterers is hardly beneficial. However, when the direct link is totally blocked, every doubling of the number of dipoles achieves almost 3 dB improvement in the received power. Hence, this low-cost and easy approach can be used as an alternative or an additional method to enhance and optimize wireless propagation channels.

REFERENCES

[1] M. A. ElMossallamy, H. Zhang, L. Song, K. G. Seddik, Z. Han, and G. Y. Li, "Reconfigurable intelligent surfaces for wireless communications: Principles, challenges, and opportunities," *IEEE Trans. Cogn. Commun. Netw.*, vol. 6, no. 3, pp. 990–1002, Sep. 2020.

[2] M. Di Renzo et al., "Smart radio environments empowered by reconfigurable intelligent surfaces: How it works, state of research, and the road ahead," *IEEE J. Sel. Areas Commun.*, vol. 38, no. 11, pp. 2450–2525, Nov. 2020.

[3] Q. Wu, S. Zhang, B. Zheng, C. You, and R. Zhang, "Intelligent reflecting surface-aided wireless communications: A tutorial," *IEEE Trans. Commun.*, vol. 69, no. 5, pp. 3313–3351, May 2021.

[4] Z. Yu, C. Feng, Y. Zeng, T. Li, and S. Jin, "Wireless communication using metal reflectors: Reflection modelling and experimental verification," in *Proc. IEEE Int. Conf. Commun.*, 2023, pp. 4701–4706.

[5] Q. Wu and R. Zhang, "Intelligent reflecting surface enhanced wireless network via joint active and passive beamforming," *IEEE Trans. Wireless Commun.*, vol. 18, no. 11, pp. 5394–5409, Nov. 2019.

[6] L. Hao, A. Fastenbauer, S. Schwarz, and M. Rupp, "Towards system level simulation of reconfigurable intelligent surfaces," in *Proc. Int. Symp. ELMAR*, 2022, pp. 81–84.

[7] S. Tretyakov, "Maximizing absorption and scattering by dipole particles," *Plasmonics*, vol. 9, pp. 935–944, 2014.

[8] F. Xia, S. Quan, and G. He, "RCS calculations of resonant dipole antennas with arbitrary loads based on the equivalent circuit method," in *Proc. 8th Int. Symp. Antennas, Propag. EM Theory*, 2008, pp. 867–870.

[9] C. A. Balanis, *Antenna Theory Analysis and Design*, 3rd ed. Hoboken, NJ, USA: Wiley, 2005.

[10] L. Hao, S. Schwarz, and M. Rupp, "The extended Vienna system-level simulator for reconfigurable intelligent surfaces," in *Proc. Joint Eur. Conf. Netw. Commun. 6G Summit*, 2023, pp. 1–6.